PNAS
www.pnas.org

Supporting Information for

From particle attachment to space-filling coral skeletons

Chang-Yu Sun[1], Cayla A. Stifler[1], Rajesh V. Chopdekar[2], Connor A. Schmidt[1], Ganesh Parida[1], Vanessa Schoeppler[3], Benjamin I. Fordyce[1], Jack H. Brau[1], Tali Mass[4], Sylvie Tambutté[5], Pupa U. P. A. Gilbert[1,6]†*

[1] Department of Physics, University of Wisconsin, Madison, WI 53706, USA.

[2] Advanced Light Source, Lawrence Berkeley National Laboratory, Berkeley, CA 94720, USA.

[3] B CUBE–Center for Molecular Bioengineering, Technische Universität Dresden, 01307 Dresden, Germany.

[4] University of Haifa, Marine Biology Department, Mt. Carmel, Haifa 31905, Israel.

[5] Centre Scientifique de Monaco, 98000 Monaco, Principality of Monaco.

[6] Departments of Chemistry, Geoscience, Materials Science, University of Wisconsin, Madison, WI 53706, USA.

† previously publishing as Gelsomina De Stasio

* Corresponding author: Pupa Gilbert
Email pupa@physics.wisc.edu

This PDF file includes:
Table S1
Figs. S1 to S5
Other Methods

Additional Supplementary files include:
Movie S1
Data files for CY1 component spectra:
A1_ACCH2O_fit_CY1.txt
A2_ACC_fit_CY1.txt
A3_Ara_fit_CY1.txt

www.pnas.org/cgi/doi/10.1073/pnas.2012025117

Table S1. The coral skeletons analyzed in Fig. 3. All species except for *Stylophora pistillata* are tropical, from the Indopacific, and reef-building. *Stylophora pistillata* is sub-tropical, from the Red Sea. For each area, the first two filenames refer to the component map (Fig. 3, panels 3-5) and its repeat, and the last two to the PIC map (Fig. 3, panels 2) acquired several hours later, once all or most minerals had crystallized.

Genus and species	clade	morphology	beam time	file name for Fig. 3	time post-mortem (hrs:min)
Acropora sp. *(As)*	Complex	Branching	Nov 2018	A194 A195 A223 A224	14:15 14:30 21:50 22:10
Blastomussa merleti (Bm)	Robust	Massive	Aug 2019	B127 B128 B140 B141	15:40 16:00 19:00 19:20
Micromussa lordhowensis (Ml)	Robust	Massive	Aug 2019	M67 M68 M103	21:20 21:40 25:25
Montipora turgescens (Mt)	Complex	Encrusting	Aug 2019	E20 E21 E59 E60	19:00 19:20 23:40 24:00
Turbinaria peltata (Tp)	Complex	Table	Jan 2018	T63 T64 T87 T88	29:00 29:20 34:10 34:30
Stylophora pistillata (Sp)	Robust	Branching	June 2016	S11 S12 S25 S26 S95 S96	29:00 29:20 35:00 35:20 28:30 29:00

Supporting Figures and Captions

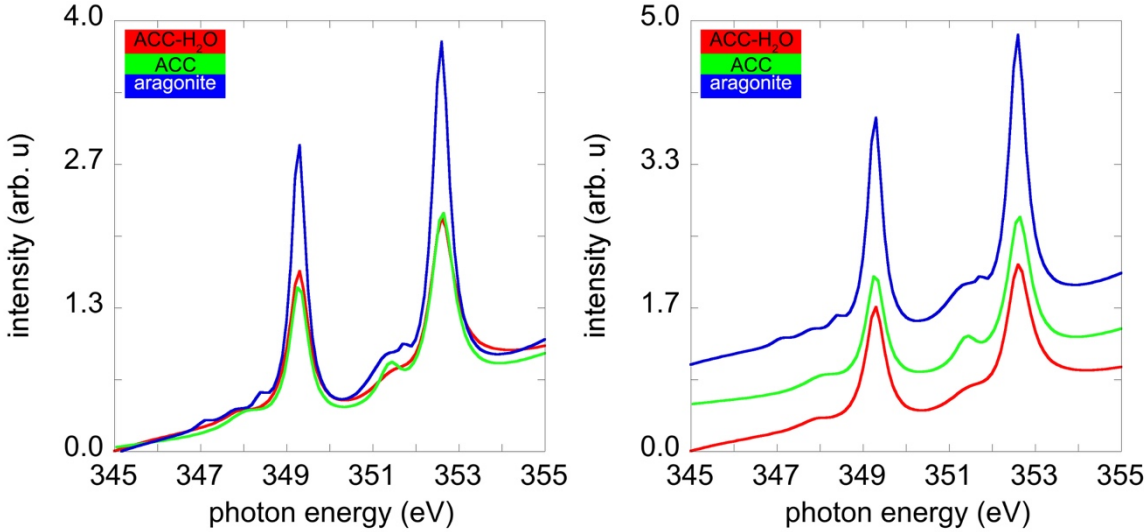

Fig. S1. The CY1 component spectra used for all component maps in this work. On the left the three components are overlapped, on the right they are displaced for clarity. Notice that in the crystalline aragonite spectrum (blue) the two main peaks are much more intense than in the amorphous precursor phases (red, green). Text files for these three spectra are provided as supporting data.

Supporting files legends:

A1_ACCH2O_fit_CY1.txt. This is a text file for the ACC-H_2O spectrum, shown above in red.

A2_ACC_fit_CY1.txt. This is a text file for the ACC spectrum, shown above in green.

A3_Ara_fit_CY1.txt. This is a text file for the aragonite spectrum, shown above in blue.

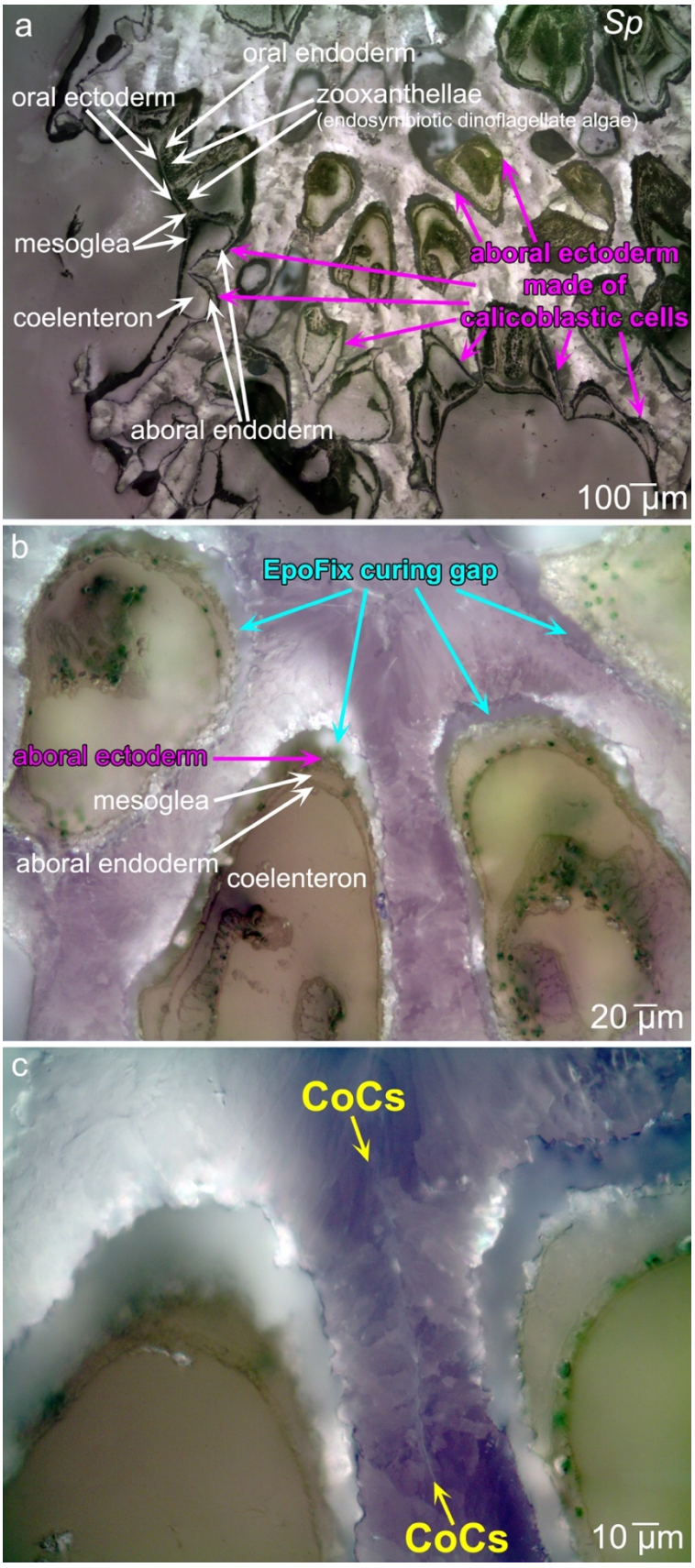

Fig. S2. Polarized light microscopy (PLM) micrographs of a *Stylophora pistillata (Sp)* area at different magnifications. Unlike the other skeletons, this one was embedded in EpoFix epoxy, not Solarez® resin. EpoFix may slightly contract in volume when curing, opening a gap between the skeleton and the EpoFix-embedded tissues.

All images in panels a,b,c were acquired with crossed polarizers, at 110° from one another. Various tissue components are labeled in panels a,b as in Fig. 2a.

Panels b,c: notice the bright regions of skeleton at the skeleton growth front. As in Fig. 2a, bright, colorful regions in polarized light are interpreted as birefringent due to nano- or micro-size anisotropic particles in the porous aggregate. In *Stylophora pistillata* the porous growth front is irregularly thick, not organized in a homogeneously thick band around the surface as in *Turbinaria peltata* (Fig. 2a).
In panel c, the centers of calcification (CoCs), arranged in a line between arrowheads at the center of a septum, show slightly higher brightness. Aragonite in the CoCs is known to be more nanoparticulate than the rest of the skeleton, and not to fill space as much as fibers (1). Lack of space filling, or nano-porosity, generating “form birefringence” is the source of the slight brightness increase observed in CoCs here.

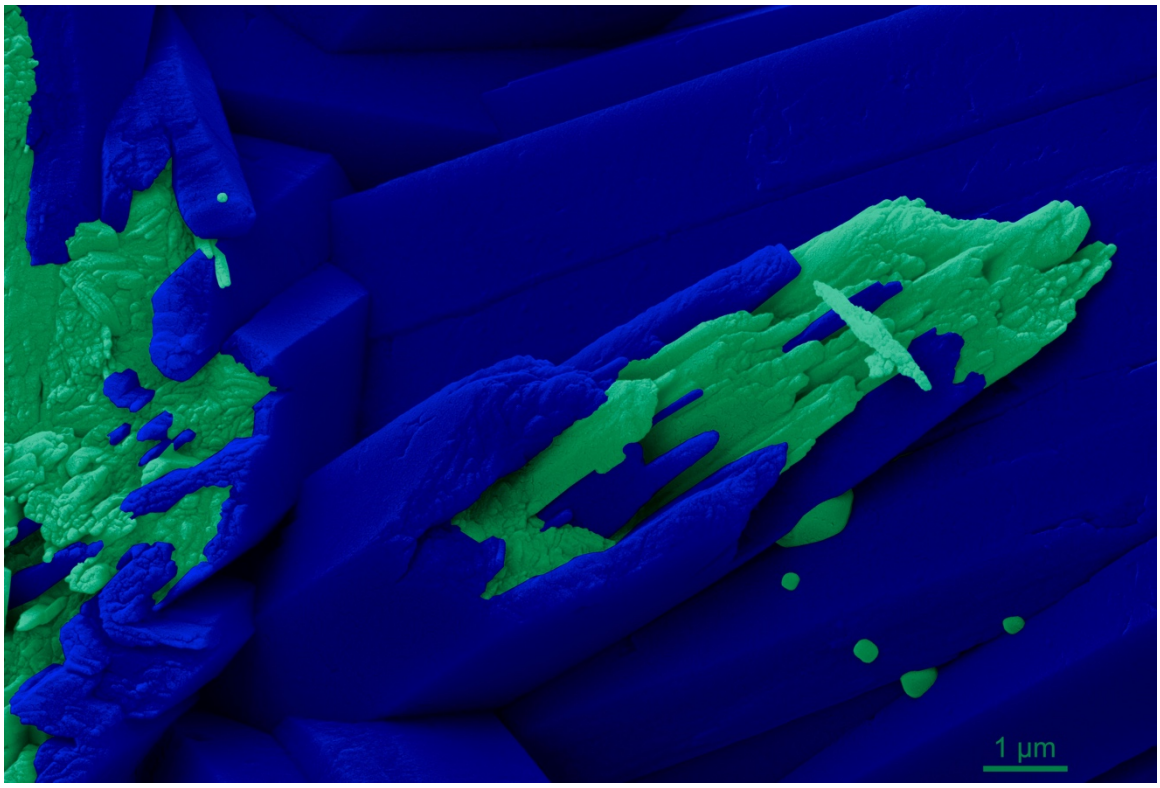

Fig. S3. Color image showing the dual mechanisms of coral skeleton fiber formation. This is the same SEM image presented as grayscale in Fig. 7b. Space-filling, euhedral crystals are false-colored in blue, non-space-filling, nanoparticle-only bearing crystals are false-colored in green. Notice that also the blue crystals have nanoparticles at their forming surfaces, and that space-filling and non-space-filling crystals are interspersed, suggesting that they may form at the same time.

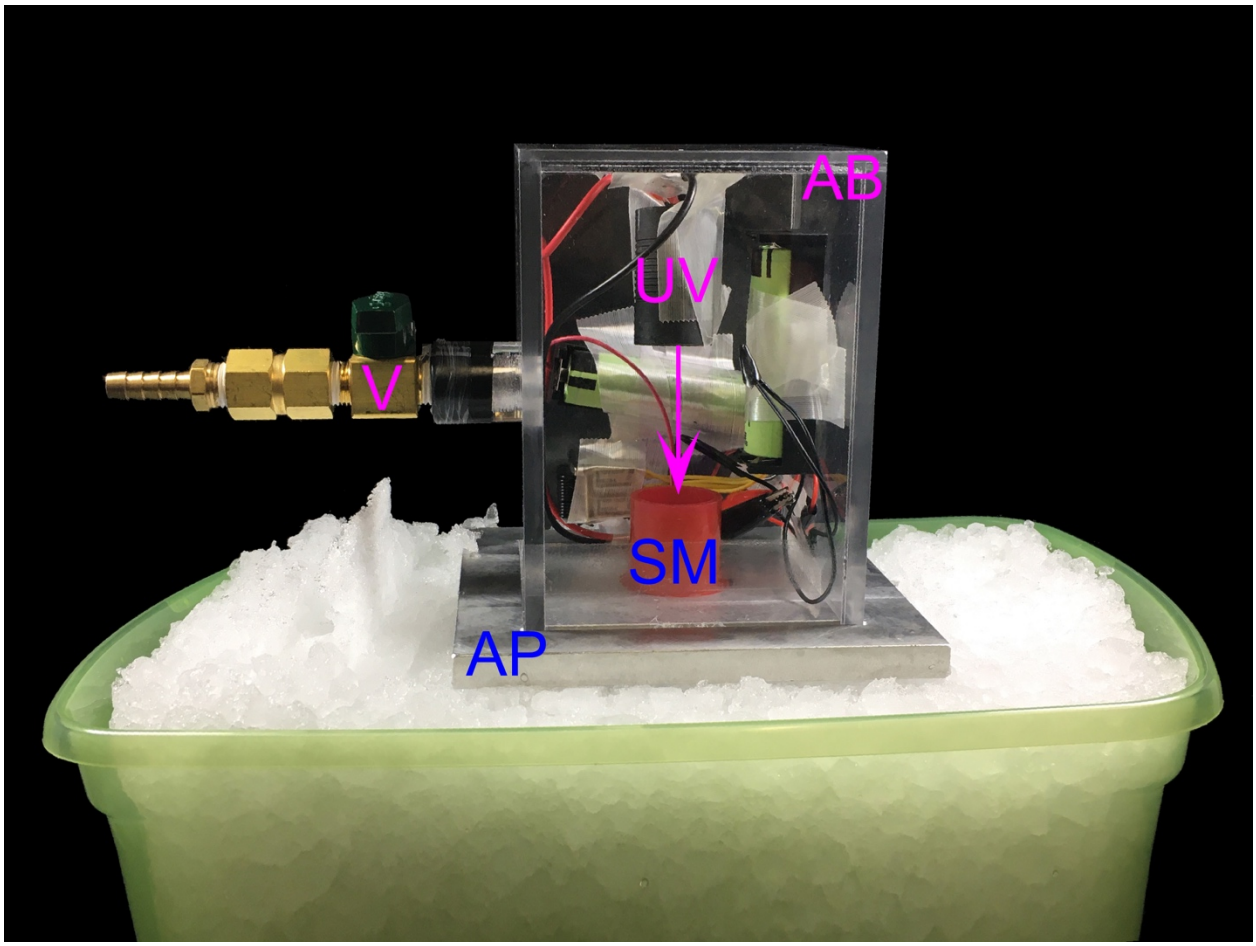

Fig. S4. The rudimentary but effective UV resin curing station for coral samples. A transparent acrylic box (AB) was sealed to the bottom aluminum plate (AP) with a Viton O-ring and evacuated. The AB contained a red plastic sample mold (SM) and a UV light, switched on and off by a remote controller. Vacuum is necessary (i) to remove air bubbles from coral sample and the Solarez® resin in which it was embedded, inside the SM, (ii) to make ethanol evaporate and be replaced by the embedding resin, and (iii) to prevent air moisture condensation onto the cold sample. After evacuating AB, the valve (V) was turned off, and AB left in static vacuum. The embedded sample was illuminated by UV light from the top (arrow). The whole station was placed on an ice tray, to keep the sample from heating during UV curing of the Solarez® resin. Movie S1 shows the remote controller in operation.

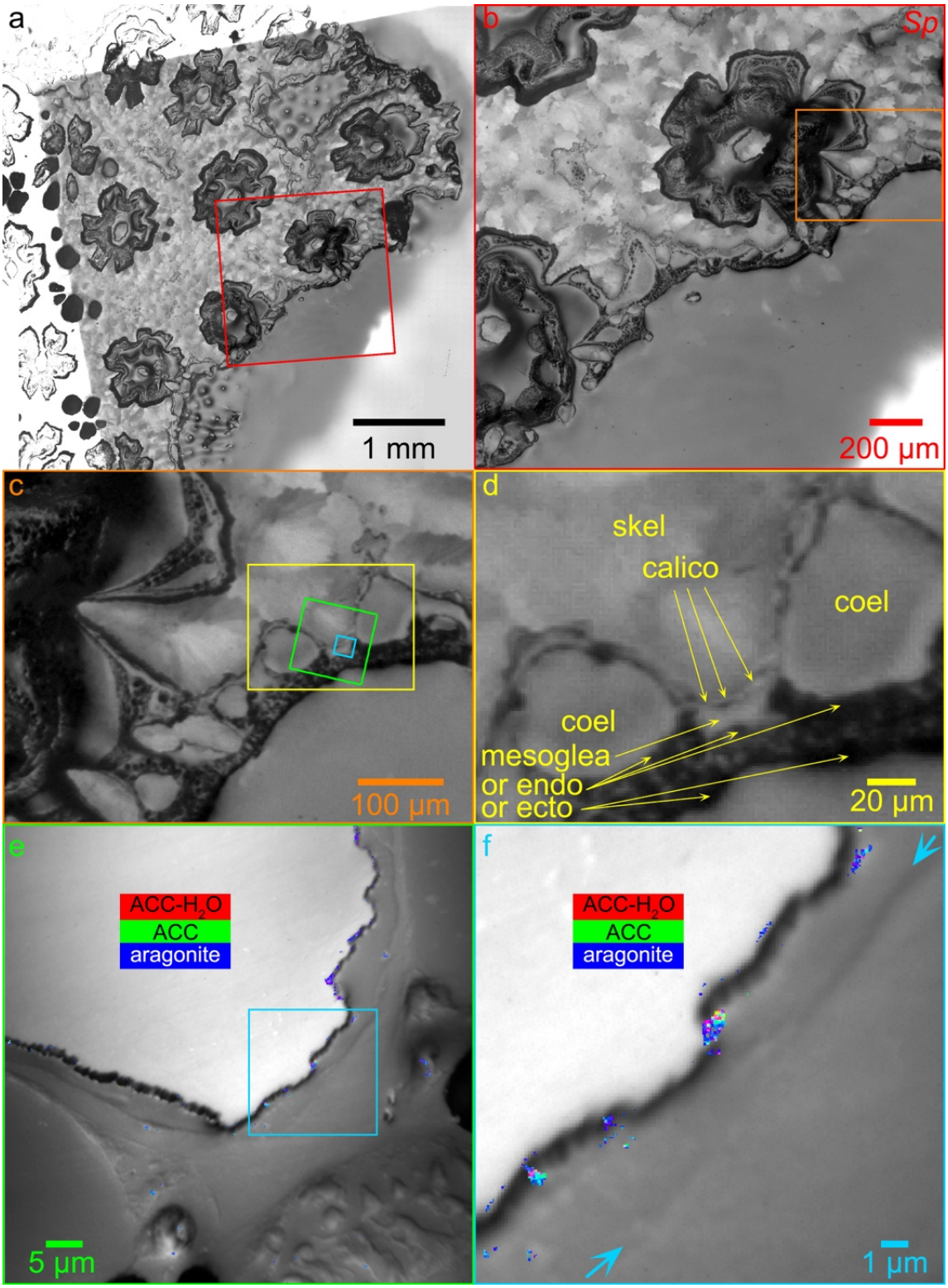

Fig. S5. Amorphous precursor particles in the calicoblastic cell layer enveloping the growing skeleton of *Stylophora pistillata*, also shown in Fig. 3G, presented here at various magnification. a-d: PLM images. D: all recognizable tissue components are labeled. Skel = skeleton, calico = calicoblastic cell layer, coel = coelenteron, mesoglea, or endo = oral endoderm containing algae, or ecto = oral ectoderm. e-f: PEEM image in grayscale and RGB component map overlaid. The

PEEM image, obtained by averaging 121 images acquired across the Ca L-edge, shows both the skeleton and the tissue components in polished cross-section. The colored pixels in the tissue indicate positions of high enough Ca concentration to be peak-fitted and displayed by component mapping. The blue pixels from the coral skeleton were removed for clarity (they are shown in Fig. 3G3). f: Magnified region from e, showing the calicoblastic cell layer as a slightly darker gray layer between the skeleton growth front and the line between two arrowheads. No cells are identifiable, possibly because this is a very thin (3nm PEEM probing depth at the Ca L-edge (2)) 2D surface of a 3D cell layer. Inside the calicoblastic cell layer Ca-rich particles contain all phases: crystalline and still amorphous 29 hours *post mortem*.

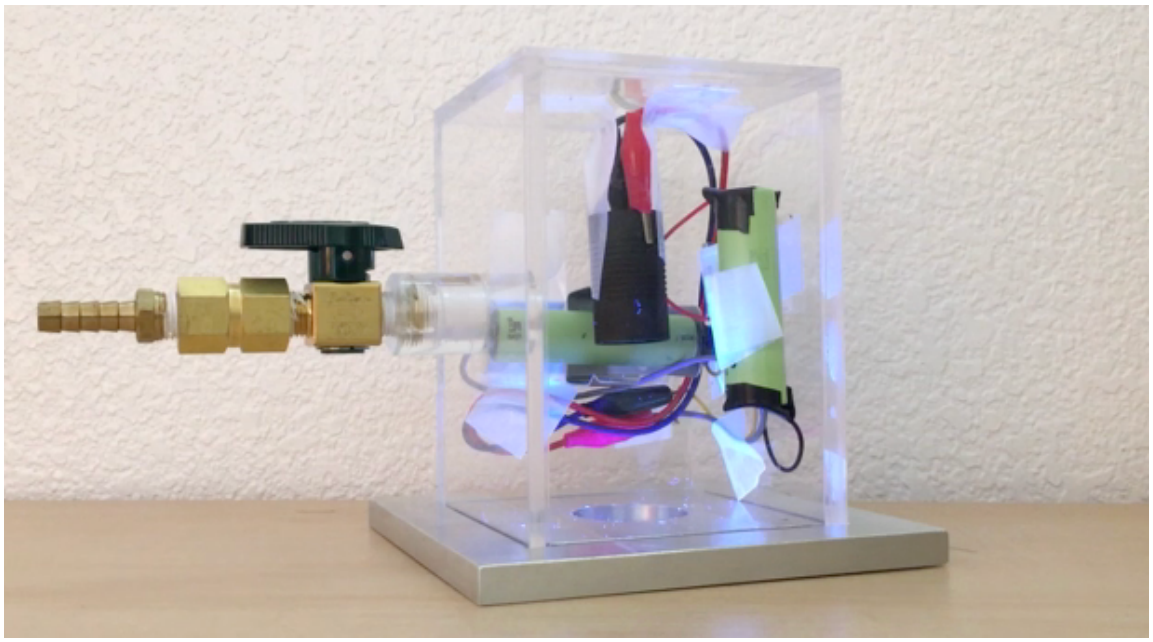

Movie S1. The movie shows the UV curing station, operated by a remote control, switching the UV light on and off. Above is a still image extracted from the movie, with the UV light on.

Other Methods

Brunauer-Emmett-Teller (BET).

Specific surface areas were measured using an Autosorb AS-1 BET instrument (Quantachrome Instruments, Boynton Beach, Florida, USA). The samples were crushed in an agate mortar and pestle and sieved through a 75-µm copper mesh. The powder collected thereafter was placed into a 9 mm glass cell, then outgassed in vacuum for ~ 2 hrs at 150 °C, to remove any moisture or gasses adsorbed onto the powder particle surfaces. The sample cells were then stabilized at liquid nitrogen temperature (77.350 °K) and measured for BET specific surface area with nitrogen gas. Multiple-point (7 points) BET surface area measurements were performed for each sample to determine its specific surface area. The seven points corresponded to p/p_o = 0.050, 0.075, 0.100, 0.150, 0.200, 0.250, and 0.300.

DNA analysis for coral species identification

All tissue samples from *B. merleti*, *M. lordhowensis*, *M. turgescens*, and *T. peltata* were fixed in pure ethanol and analyzed at the University of Haifa, Israel. Genomic DNA was extracted using the Wizard® Genomic DNA Purification Kit (Promega, USA). The PCR amplifications were performed using GoTaq® Green Master Mix (Promega, USA) using the following primers - FOL-LDEG (forward) 5'- TCWACHAAYCATAARGAYATWGG -3' and FOL-HDEG (reverse) 5'-TAAACYTCDGGRTGCCCAAARAAYCA -3' (modified from (3) The resulting OTUs sequences were aligned with ClustalX (4) and blasted on GenBank (5). The *Acropora* sample was identified only by the distinctive morphology of this genus, but the species is uncertain.

SEM analysis of coral skeletons

All coral skeletons analyzed at the SEM were precisely the same as those analyzed with PEEM, and were thus fixed and dehydrated, but not embedded. Two-three millimeter-size fragments were fractured using diagonal cutting pliers, in air, at room temperature, mounted on SEM stubs with carbon tape (Ted Pella, Redding, CA), and coated using a high-resolution Cressington 208hr sputter coater with rotary, planetary, and tilting movements (Cressington, UK), which is optimized for coating distribution and coverage of highly topographic coral skeletons. We coated with 20 nm Pt while rotating and tilting the samples. These preparations were done in the Gilbert lab, Chamberlin Hall, University of Wisconsin, Madison, WI, USA. The samples were then analyzed by PG and TM via teleconferencing (during the Pandemic, in May and June 2020), at the University of Haifa, Israel. The microscope used for Figs. 1, 5, 7 was a Zeiss FE-SEM SIGMA HD, operated in secondary electron mode, with 10 kV accelerating voltage, with magnifications 50,000x, 10,000x, 1,000x, and 250x for each area analyzed.

False-coloring of SEM image

The SEM image in SI Appendix Fig. S3 was false-colored using Adobe Photoshop®, version CC 2017. The same image is presented as the original grayscale image in Fig. 7b. The false-color image was created by converting the image to a blue tritone, then to a green tritone, and the two were overlapped as separate Photoshop layers. The green one was then cutout using the eraser, to remove all the space-filling parts.

References

1. Benzerara K*, et al.* (2011) Study of the crystallographic architecture of corals at the nanoscale by scanning transmission X-ray microscopy and transmission electron microscopy. *Ultramicroscopy* 111(8):1268-1275.
2. Frazer BH, Gilbert B, Sonderegger BR, & De Stasio G (2003) The probing depth of total electron yield in the sub keV range: TEY-XAS and X-PEEM. *Surf Sci* 537:161-167.
3. Vrijenhoek R (1994) DNA primers for amplification of mitochondrial cytochrome c oxidase subunit I from diverse metazoan invertebrates. *Mol Mar Biol Biotechnol* 3(5):294-299.
4. Larkin MA*, et al.* (2007) Clustal W and Clustal X version 2.0. *bioinformatics* 23(21):2947-2948.

5. http://www.ncbi.nlm.nih.gov/BLAST